Int. J. Multiphase Flow Vol. 15, No. 5, pp. 735–746, 1989
Printed in Great Britain.

0301-9322/89 $3.00 + 0.00

PARTICLES–TURBULENCE INTERACTION†

G. HETSRONI‡
Department of Mechanical Engineering, Technion—Israel Institute of Technology, Haifa, Israel

(*Received* 28 *April* 1989)

Abstract—The interaction between solid particles and the turbulence of the carrier fluid is considered. Theoretical considerations suggest that particles with low Reynolds number cause suppression of the turbulence, while particles with higher Reynolds number cause enhancement of turbulence due to wake shedding. A review of the available experimental data supports this observation.

Key Words: two-phase flow, turbulence, pneumatic transport

INTRODUCTION

In 1971, I thought that we understood the interaction between small particles and the turbulence structure of the carrier fluid. The experimental evidence which we then had (Hetsroni & Sokolov 1971) was clear enough . When I was invited to give this lecture about a year ago, I already knew better—but I thought that the time was sufficient to sort out all the literature in this complex subject and come up with some simple unified theory. Since then, I have found that there is a recent voluminous literature on the subject—unfortunately not all of it is useful, or even correct.

Here I will consider the interaction between turbulent fluid flow and the particles which are suspended in the flow. This topic is of considerable theoretical interest since it may be helpful in the understanding of turbulence dynamics. There may, in the future, be some practical application to this study—say for turbulence control, such as drag reduction. Since there is a very large number of variables which may affect this interaction, I will limit the discussion to solid (or almost solid) particles of sizes in the range 10–3000 μm. That way, we eliminate the effects of the uncertain geometry of the interfaces (as with bubbles) and also the elastic properties (due to surface tension) of the bubbles. We also eliminate the effect of Brownian motion. Yet, we retain the important effect of the particles on energy-containing eddies, which is the basic phenomenon which we want to examine.

Our discussion will start with some order of magnitude consideration, followed by a review of experimental data which were published in the literature. We make in this discussion the usual assumptions, i.e. that the fluid is Newtonian, the mean flow is steady and that the particles are monodisperse (i.e. of the same size).

The interaction between the particles and the fluid is based on their size, relative velocity and the difference in densities, and can best be correlated by a Reynolds number

$$\mathrm{Re}_\mathrm{p} = \frac{(u_\mathrm{f} - u_\mathrm{p})d(\rho_\mathrm{p} - \rho_\mathrm{f})}{\mu_\mathrm{f}} = \frac{u_\mathrm{R}\, d(\rho_\mathrm{p} - \rho_\mathrm{f})}{\mu_\mathrm{f}}, \qquad [1]$$

where u are the velocities and ρ are the densities of the fluid f and particle p, respectively; d is the diameter of the particle, μ_f is the viscosity of the fluid and u_R is the relative velocity between the particle and surrounding fluid. Equation [1] is not the conventional definition of particle Reynolds number, as is given in [5]—yet, since inertia and buoyancy forces play a major role in particle dynamics, this definition must be useful.

†Based on an Invited Lecture, *ASME Winter Annual Meeting*, Chicago, Illinois, 1988.
‡Currently a Visiting Professor at: Department of Chemical and Nuclear Engineering, University of California, Santa Barbara, CA 93106, U.S.A.

The other important parameter which can be used to characterize the particles is the relaxation time t^*, i.e. the time it takes for a particle at rest to be accelerated within ~63% of the fluid velocity. A simple force balance will show that the relaxation time is

$$t^* = \frac{d^2 \rho_p}{18 \nu_f \rho_f}. \qquad [2]$$

This relaxation time is strictly correct only for Stokes' regime, when $Re_p < 1$. For larger Reynolds numbers, the drag coefficient is much higher than that predicted by Stokes' law, and [2] would overestimate the relaxation time. Since our discussion is limited to order of magnitude estimation, we will not seek a more precise expression. The relaxation time of the particle has to be compared with a characteristic eddy turnover time. The characteristic time of eddies is their characteristic size l_e divided by some characteristic velocity u_e:

$$t_e = \frac{l_e}{u_e} = \frac{2\pi}{\tilde{k} u_e}, \qquad [3]$$

where $\tilde{k}$ is the wavenumber.

For a single-phase jet, Wygnanski & Fiedler (1969) showed that $l_e/x = 0.081$, where l_e is defined as the integral length scale and x is the axial distance from the nozzle. For pipe flow, the scale of the energetic eddies is of the order of $0.1R$ (R is the pipe radius). Hutchinson *et al.* (1971) measured the length scale and found it to be $l_e/R \approx 0.2$ over most of the pipe diameter, decreasing to close to zero for radial locations between about 0.7 of the radius and the pipe wall.

ORDER OF MAGNITUDE CONSIDERATIONS

Owen (1969) used order of magnitude considerations to suggest how the relative motion of particles affects the turbulence of the mainstream. Very small particles were postulated to follow the motion of the fluid very closely—the smaller the particles are, the closer they follow the motion of eddies of higher frequency. One can get an idea as to how small is small from figures 1(a) and 1(b). The figures show the velocities of particles of various sizes, as measured in an air flow behind a backward-facing step flow.

In figure 1(a), the maximum positive velocity (normalized with respect to the maximum approach velocity u_0) is depicted for particles of 1, 15 and 30 μm dia. If one assumes that the 1 μm particles follow the motion of air quite closely, the particles of 15 μm dia already deviate from the motion of the smaller particles. The phenomenon becomes more pronounced as the particle size increases. In the current study only particles up to 70 μm were measured.

In figure 1(b), similar phenomena can be noted; i.e. one can observe that particles of 15 μm and larger lag behind the motion of the air, and the difference in velocities increases as the particles' diameter increases.

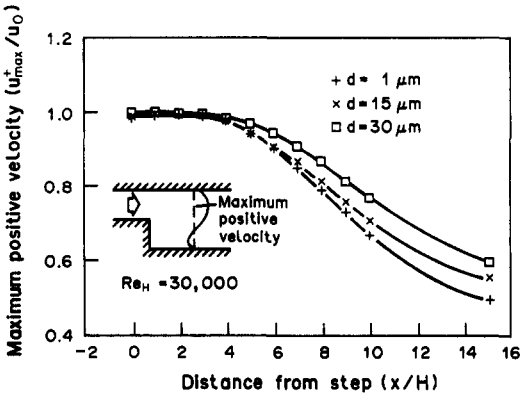

Figure 1a. Maximum positive velocity u^+_{max} (normalized with u_0) in the streamwise portion of the velocity profile of particles of different sizes. u_0 is the maximum approach velocity (Ruck & Makiola 1989).

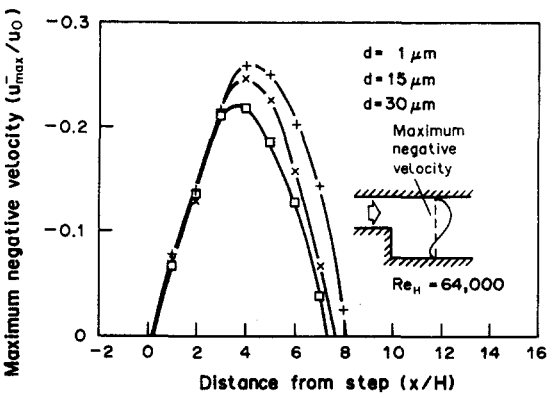

Figure 1b. Maximum negative velocity u^-_{max} (normalized with u_0) in the recirculation zone of particles of different sizes (Ruck & Makiola 1989).

For example, Hetsroni & Sokolov (1971) used oil droplets of the order of 13 μm in an air jet. (Note that droplets of this size act almost as solid particles.) Their jet was issued from a 25 mm nozzle at velocity of about 60 m/s, and the characteristic size of the energy-containing eddies at $x = 30D$ is $l_e \approx 6$ mm; thus, the droplets would have very little effect on the energy-containing eddies, which was indeed observed experimentally.

For these small particles, where $t^* \ll t_e$, the rate of turbulent energy dissipation is increased, compared to single-phase flow, by a ratio of $(1 + m/\rho_f)^{1/2}$, where m is the loading, i.e. the mass concentration of particles. Thus, at the subenergetic range, the particles extract energy from the flow and dissipate it.

The response of the particles to the motion of the fluid becomes imperfect when their characteristic time t^* is of the same order of magnitude as the characteristic time of the eddies—namely, the particles follow the motion of eddies of decreasing frequency as their sizes increase, or as $t^* \approx t_e$, i.e. if the characteristic scale of the energetic eddies in pipe flow is $0.2R$, then

$$t^* \approx \frac{0.2R}{u_\tau}, \qquad [4]$$

where $u_\tau = \sqrt{\tau_w/\rho}$ is a characteristic velocity in the pipe, say the friction velocity.

For larger particles, $t^* > t_e$, Owen (1969) suggested that the turbulent fluctuations in the presence of particles should decrease as $[1 + (m/\rho_f)(t_e/t^*)]^{-1/2}$, compared with the particle-free stream. For larger particles, where $t^* \gg t_e$, the particles are sensitive to turbulent fluctuations only of very low frequency (or high wavenumber), and they possess a higher mean velocity relative to the fluid. Experimental data actually suggests that the turbulence in the mainstream is *enhanced* by the presence of these particles, as we shall see below.

TURBULENCE ENHANCEMENT

The enhanced turbulence in the presence of large particles could be explained by the vortex shedding phenomenon. Indeed, it is known that when

$$\tilde{\mathrm{Re}}_p = \frac{(u_f - u_p)d}{\nu_f} \leqslant 110 \qquad [5]$$

(notice that this definition is somewhat different than [1]), there is no vortex shedding downstream of the particle. Achenbach (1974) has shown that vortex shedding occurs as $\tilde{\mathrm{Re}}_p > 400$. In his experiments vortex shedding occurred in the range $400 < \tilde{\mathrm{Re}}_p < 1000$, with a Struhal number $\mathrm{S} = 0.2$ ($\mathrm{S} = fd/u_f$; f—frequency of vortex shedding, d—diameter of sphere, u_f—free stream velocity). For $1000 < \tilde{\mathrm{Re}}_f < 10{,}000$, he found that $\mathrm{S} = 2.0$.

An examination of the data by Tsuji *et al.* (1984, 1988; Tsuji & Morikawa 1982) (figure 2) reveals that small particles, $d = 200\ \mu$m, $\tilde{\mathrm{Re}}_p \approx O(0.10)$, always caused suppression of the turbulence of the mainstream. Larger particles, $d = 300\ \mu$m, $\tilde{\mathrm{Re}}_p \approx O(1000)$ always caused an increase in the turbulence intensity in the mainstream (figure 3). The particles with $d = 500\ \mu$m and $\mathrm{Re} \approx O(100)$ had a mixed effect on the turbulence of the mainstream. They tended to increase the turbulence in the central part of the pipe, and suppress it in the region $0.5 < r/R < 1.0$. In the next section the available experimental data will be reviewed. With typical values, $d = 200\ \mu$m, $u_R \approx 2$ m/s, $\nu_f = 16 \times 10^{-6}$ m^2/s, we find $\tilde{\mathrm{Re}}_p = 25$, i.e. these particles will tend to suppress the turbulence, as indeed is observed in figure 8(a). With typical values $d = 3000\ \mu$m, $u_R \approx 10$ m/s, $\nu_f = 16 \times 10^{-6}$ m^2/s, we find $\tilde{\mathrm{Re}}_p = 625$, i.e. we would expect to see vortex shedding with $s = 0.2$ or frequency $f = 667$. This is in the frequency range where one would expect to observe a considerable effect on the turbulence intensity.

EXPERIMENTAL DATA

There are very few good experimental data sets on the interaction between particulate matter and the turbulence of the mainstream. The reason for the paucity of data is that the experiments are very difficult to conduct!

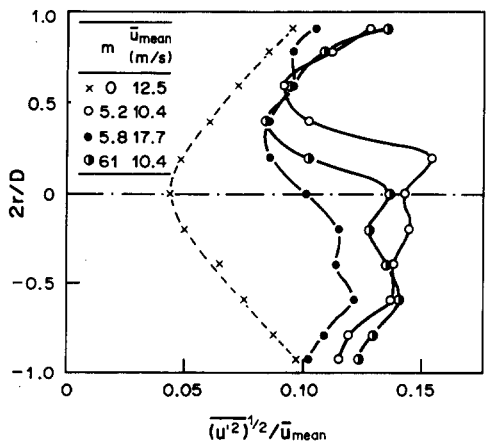

Figure 2. Turbulence intensity of air in the presence of 3.4 mm particles in a 30 mm dia horizontal pipe (Tsuji & Morikawa 1982).

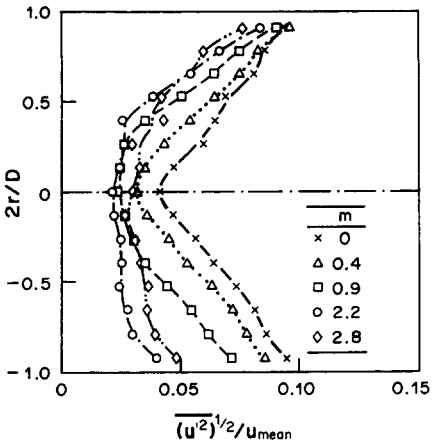

Figure 3. Turbulence intensity of air in the presence of 0.2 mm particles in a 30 mm dia horizontal pipe $\bar{u}_m = 15$ m/s (Tsuji & Morikawa 1982).

Early experiments (e.g. Hetsroni & Sokolov 1971; Serizawa 1974; Serizawa & Kataoka 1980; Serizawa *et al.* 1975) used hot-wire anemometry with special techniques to filter out the effect of the droplets (or bubbles) on the hot wire. These data have been criticized (Faeth 1983, 1987), claiming that only a relatively small fraction of the drops which impinged on the hot wire were accounted for, which tended to bias the results. Though it is, admittedly, possible that some bias existed, the results are still considered valid—in particular, the energy spectra (figure 4), which could not have been biased in this manner. Later measurements were all conducted with a laser-Doppler anemometer—an experimental technique which is not without difficulties. Actually, there are only six sets of data of fluid–solid flow in a pipe, and most of them are not detailed enough for any definitive conclusions to be drawn. Other data were obtained using a free jet, a geometry which is experimentally much more convenient than a tube. In table 1 (Gore & Crowe 1989), all available experimental data are summarized. In the table, the geometry is given together with the ratio of the density of the particle ρ_p to the density of the fluid ρ_f, particle volume fraction c%, and the fluid's Re, i.e. the mainstream's Reynolds number. In the table there are sets of gas–solid, liquid–solid and gas–liquid data. The latter set was included because the very small liquid droplets in air behave very much as solid particles in air.

Other data sets (e.g. Snyder & Lumley 1971; Wells & Stock 1983) did not include measurements of turbulence as such (they measured only diffusivity), and are not included in table 1.

It would be best now to plot the change in turbulence of the fluid, as a function of the local $\tilde{Re}_p$ in order to get a clear indication of the effect of the particles on the turbulence of the mainstream. Unfortunately, not all of the data sets enables an exact calculation of the local $\tilde{Re}_p$,

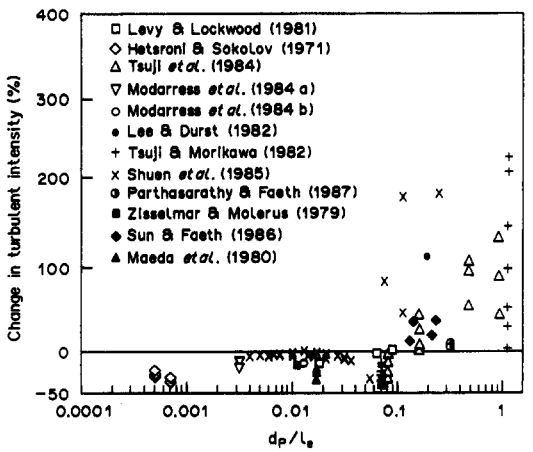

Figure 4. Change in turbulence intensity as a function of the length scale ratio (Gore & Crow 1989).

Table 1. Experimental parameters

Reference	Geometry	$\frac{\rho_p}{\rho_f}$	C	Re_f
Levy & Lockwood (1981)	Gas–solid downward jet	2000	6×10^{-4}	20,000
Hetsroni & Sokolov (1971)	Gas–liquid horizontal jet	775	2.5×10^{-6}	83,300
Tsuji *et al.* (1984)	Gas–solid upward pipe	850	5×10^{-3}	22,500
Modarress *et al.* (1984a)	Gas–solid downward jet	2500	2×10^{-4}	13,300
Tsuji & Morikawa (1982)	Gas–solid horizontal pipe	833	4×10^{-3}	20,000
Shuen *et al.* (1985)	Gas–solid downward jet	2200	2×10^{-4}	19,000
Parthasarathy & Faeth (1987)	Liquid–solid downward jet	2.5	2.4–4.8	9000
Modarress *et al.* (1984b)	Gas–solid downward pipe	2500	3.5×10^{-4}	17,000
Lee & Durst (1982)	Gas–solid upward pipe	2080	1×10^{-3}	8000
Zisselmar & Molerus (1979)	Liquid–solid horizontal pipe	2.5	4.0	100,000
Maeda *et al.* (1980)	Gas–solid upward pipe	7500	1×10^{-4}	20,000

because the relative velocity is unknown. One could present the data as the change in turbulence due to the particles, as a function of the relative size of the particles, i.e. the ratio of the particle size to a characteristic length scale of the system. The characteristic length scale of the energy-containing eddies was taken as $0.2R$ at the pipe center and $0.05R$ or so near the wall (Hutchinson *et al.* 1971). For a single-phase jet, the data of Wygnanski & Fiedler (1969) that $l_e/x = 0.081$, where x is the axial distance from the exit nozzle, was used.

The percentage change in turbulence intensity is defined in figure 4 (Gore & Crowe 1989) as

$$\frac{\sigma_{TP} - \sigma_f}{\sigma_f} \times 100,$$

where $\sigma = \sqrt{\overline{u'^2}}/u$ is the turbulence intensity, the subscript TP is for two-phase and f is for fluid.

Some typical sets of data are now demonstrated, first in jets and then in pipe flow.

Jets

In one of the earliest measurements (Hetsroni & Sokolov 1971), the properties of an air jet laden with 13 μm droplets were measured. The jet was issued from a 25 mm round nozzle with a velocity of 50–60 m/s. The intensity of turbulence $\sqrt{\overline{u'^2}}/u_m$ (where u_m is the maximum longitudinal velocity in the cross section) was uniformly reduced by the small particles (figure 5), i.e. it was decreased

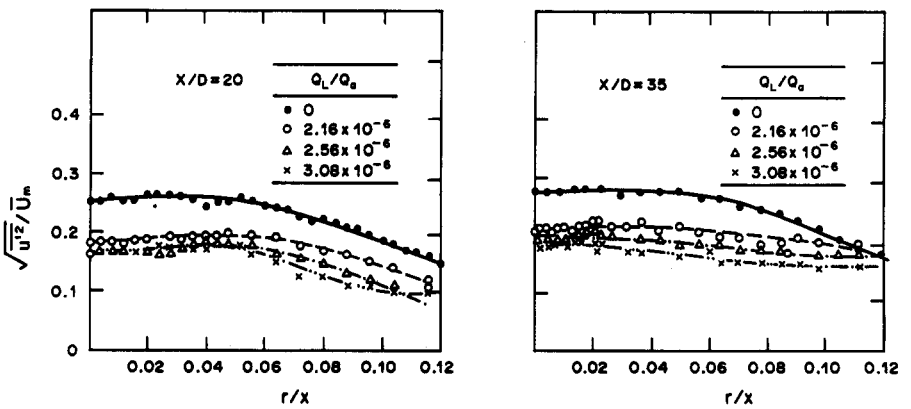

Figure 5. Distributions of the intensity of turbulence of longitudinal velocities across the jet, at $x/D = 20$ and 35, for various concentrations of droplets (Hetsroni & Sokolov 1971).

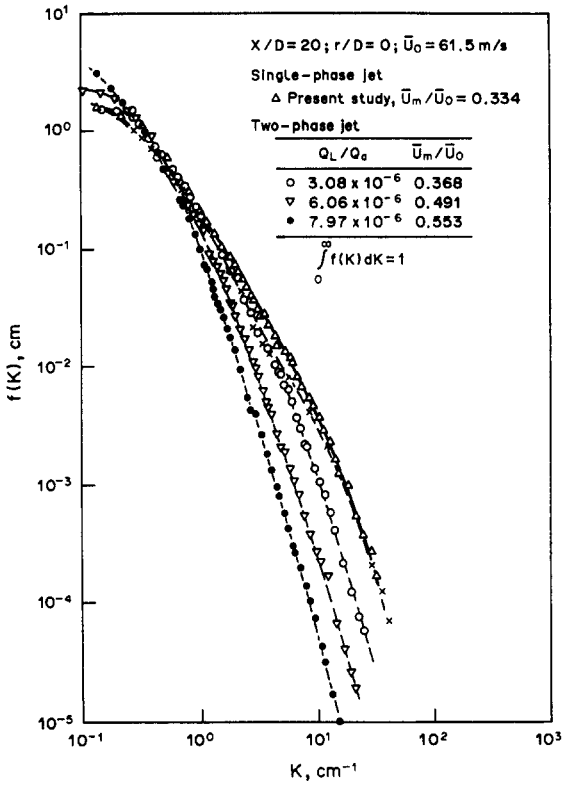

Figure 6. One-dimensional energy spectra of longitudinal velocity fluctuations for single- and two-phase jets (Hetsroni & Sokolov 1971).

almost proportionally to the loading of droplets (Q_c is the volumetric flow rate of the droplets and Q_a is the volumetric flow rate of the air). Notice that the droplets are rather small and the loading was relatively light. The spectra of turbulence, which are shown in figure 6, indicate that the particles decrease the spectral components at high frequency (K is the wavenumber, cm^{-1}), defined as $2\omega/(100\,u_m)$ where ω is the frequency and u_m is the centerline time-averaged velocity in m/s.

Tsuji *et al.* (1988) used a one-dimensional LDA to measure the motion of particles in an air jet. Their data show the effect of coarse particles on the turbulence of an air jet. The intensity of turbulence ($Tu = \sqrt{\overline{u'^2}}/u_0$, where u_0 is the velocity at the nozzle) at the jet axis, when the jet was laden with particles of three sizes, is depicted in figure 7. The effect of the 170 μm particles is to decrease the intensity of turbulence. There is very little effect of the large particles—primarily because the loading is very light—but it seems that they increase the intensity of turbulence at least in some parts of the jet, i.e. from $x/d \approx 5$ to $x/d \approx 10$.

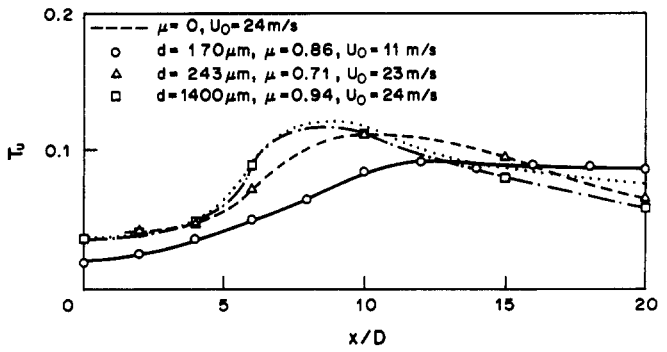

Figure 7. Variation of the centerline turbulence intensity of an air jet loaded with particles of various sizes (Tsuji *et al.* 1988).

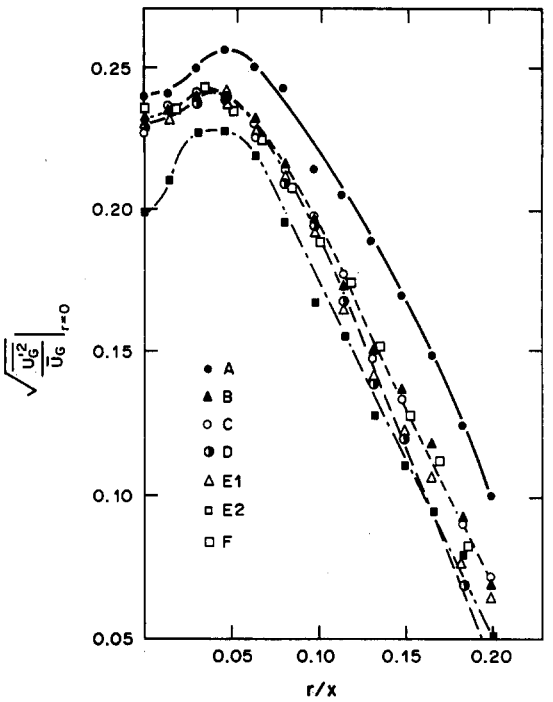

Figure 8. r.m.s. Axial air velocity of an axially symmetrical jet loaded with particles of various sizes, at $x = 20D$ (Levy & Lockwood 1981).

Code	Particle size range (μm)	Air flow rate (kg/s)	Sand flow rate (kg/s)	Sand-to-air ratio	$\bar{u}_c$ at $r = 0$ and x = 20D	$\bar{u}_p$ at $r = 0$ and x = 20D
A	850–1200	4.29×10^{-3}	15.0×10^{-3}	3.5	7.3	8.74
B	600–850	3.62×10^{-3}	8.78×10^{-3}	2.42	6.12	8.20
C	380–700	3.62×10^{-3}	8.12×10^{-3}	2.24	6.0	8.52
D	300–500	3.62×10^{-3}	4.42×10^{-3}	1.22	8.79	13.22
E1	180–250	3.62×10^{-3}	4.13×10^{-3}	1.14	9.06	14.90
E2	180–250	3.62×10^{-3}	8.45×10^{-3}	2.33	7.57	11.55
F	Clean gas	4.29×10^{-3}	—	—	9.6	—

Levy & Lockwood (1981) used a one-dimensional LDA to measure sand particles in a free downward air jet. In figure 8 (Levy & Lockwood 1981), these trends are more clear. Here too, the turbulence (actually the r.m.s. of the axial velocity normalized to the time-averaged axial velocity) is plotted for various sizes of sand particles vs the radial position at $x = 20D$. Clearly, the larger particles of 850–1200 μm (A in the figure) cause a significant increase in turbulence level, whereas the smaller particles of 180–250 μm (E in the figure) clearly cause a suppression of the turbulence. The particles of inbetween sizes had a mixed effect.

Parthasarathy & Faeth (1987) measured and calculated a particle-laden water jet. They used a two-beam forward-scatter laser for particle velocity measurement. The particle signals were discriminated from the signals of the naturally seeded water, based on their amplitude. Their experimental results are depicted in figure 9. Their particles were glass beads $\rho_p = 2450$ kg/m^3 and diameter (SMD) = 505 μm. Effects of turbulence modulations can be observed, evidenced by increased turbulence levels near the axis, where turbulence production by conventional continuous-phase mechanisms is small. The phenomenon did not appear to influence the overall mixing and turbulent dispersion of the flow, since effects of particles on continuous phase turbulent properties are probably limited to wavenumbers which are higher than the energy-containing range of the turbulence spectrum, which is largely responsible for mixing. It is worthwhile noticing that while the kinetic energy k of the turbulence is somewhat increased in the two-phase jet, as compared to the single-phase one, the cross correlation $\overline{u'v'}$ is decreased. The latter, maybe, points to the fact that because of inertia and crossing trajectories effect, the particles fall from one eddy to another, so that the correlation between particle and fluid velocities decreases, which affects the cross correlation of the fluid.

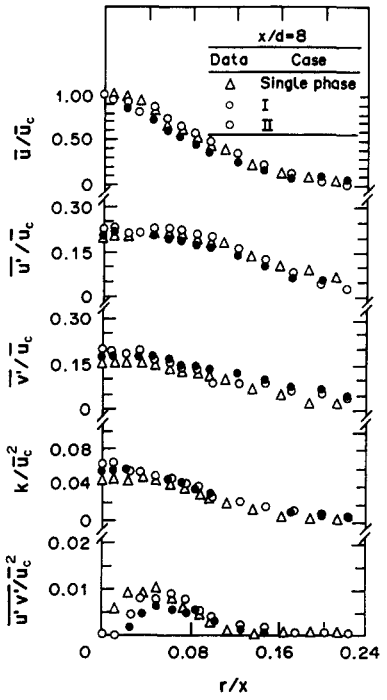

Figure 9. Mean and turbulent liquid properties in a particle-laden water jet at $x/d = 8$ (Parthasarathy & Faeth 1987).

Pipe flow

Although two-phase flow in pipes has been of interest for a long time (pneumatic conveying), there has been almost no experimental data, until very recently, on the structure of turbulence. Owen's (1969) excellent review on pneumatic conveying includes a discussion on turbulence, but he did not have the experimental data to support it.

The first detailed measurements are those of Tsuji & Morikawa (1982), where plastic particles of dia 200 μm and 3.4 mm and density $\rho_p = 1000\ \mathrm{kg/m^3}$, were conveyed in a horizontal pipe of 30 mm dia. They observed an increase in velocity asymmetry as the loading ratio increased up to 6, and the air velocity decreased. In the presence of 200 μm particles, a flattening of the velocity profile was observed. The large particles caused a marked increase in turbulence levels, while the small particles reduced it. The probability density function also deviated from the normal, in the presence of particles. The effect of gravity resulted in an asymmetry of particle concentration which, in a way, helps to understand the phenomenon. The distribution of turbulence intensity $\sqrt{\overline{u'^2}}/u_m$ of air flow in the presence of 3.4 mm particles is depicted in figure 2. The curves indicate a large increase in the turbulence intensity, which is caused by the particles. The increase is not symmetrical, since the concentration of the particles is asymmetric because of the gravity effect. The particle Reynolds number was estimated to be 470—namely in the range where vortex shedding occurs.

In figure 3, the turbulence intensity of the air in the presence of 200 μm particles is depicted. It is quite obvious that the turbulence is suppressed for all particle loadings m.

Verticle pipe flow was investigated by Tsuji *et al.* (1984). They used four sizes of plastic particles, 200 μm to 3 mm, in a 30 mm vertical pipe. The smaller the particles, the flatter was the mean velocity distribution (figure 10). Again, as seen in figure 11, large particles (possessing a high Reynolds number) increased air turbulence throughout the pipe cross section, while small particles (with a low Reynolds number) reduced it. In medium-sized particles, both effects were observed—turbulence was increased around the pipe center and reduced near the walls.

Tsuji *et al.* (1984) also measured the energy spectra with the various particles. They found that the spectra were not influenced by large particles, while the smaller particles caused a flattening of the profiles. The latter result is contrary to the result of Hetsroni & Sokolov (1971) and to various theoretical analyses, and cannot be explained now.

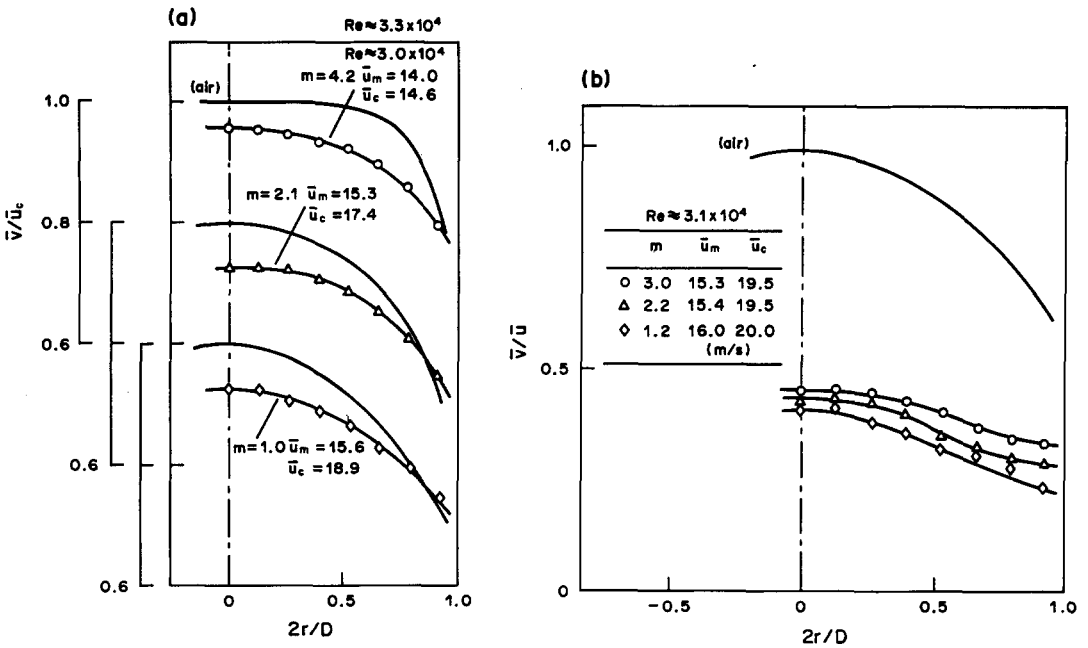

Figure 10. Mean air and particle velocity distributions in a vertical pipe, in the presence of (a) 200 μm plastic particles and (b) 3 mm particles (Tsuji *et al.* 1984).

Nouri *et al.* (1987) measured flow characteristics in descending solid–liquid turbulent flow in a vertical tube, with spherical particles with a mean dia 270 μm (100–500 μm) at concentrations 0.1–14%. They also found that the fluctuating velocities of the particles are always smaller than those of the single phase by about 5% on the axis and 13% near the wall. The fluctuations of the particles' velocities decreased with increasing concentrations, namely they affected the mainstream more.

Lee & Durst (1982) showed that 800 μm glass beads increased the turbulence over the entire cross section, similar to the 3 mm particles which Tsuji *et al.* (1984) used. The reason (maybe) is that the glass beads had a density of $\rho_p = 2600$ kg/m^3, while the plastic particles had $\rho_p = 1000$ kg/m^3. It is interesting to note that Lee & Durst (1982) and Tsuji *et al.* (1984) found that for small particles (~ 200 μm), there is a point at approx. $r/R \simeq 0.8$ where the mean particle velocity is higher than the mean fluid velocity. For larger particles (> 500 μm), no such point was found. No such point was found in the investigation of Maeda *et al.* (1980), even though they used particle sizes < 200 μm

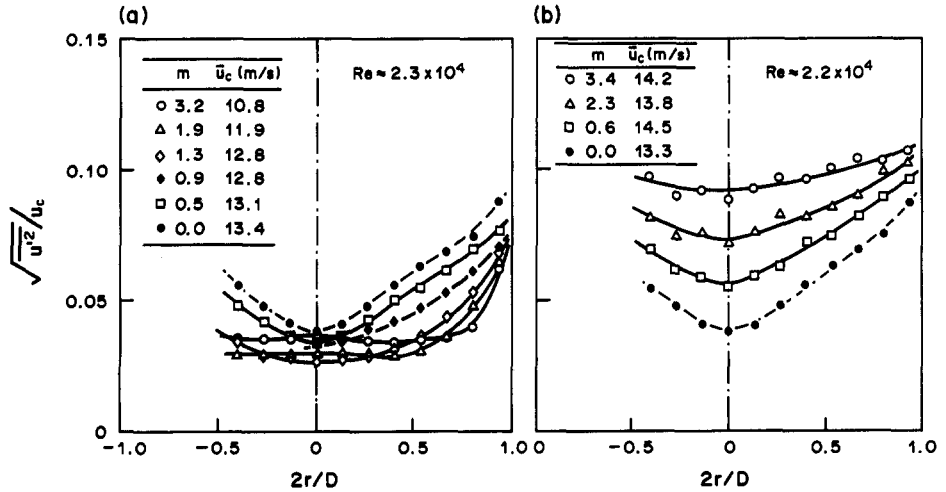

Figure 11. Turbulence intensity of air vertical pipe flow, in the presence of (a) 200 μm particles and (b) 3 mm plastic particles (Tsuji *et al.* 1984).

and density ratios which are approximately equivalent to those used by Tsuji *et al.* (1984) and Lee & Durst (1982).

Here we examined only particle–fluid interaction. The particle–particle interaction may become more important as the loading increases. The particle–wall interaction is, of course, important close to the wall. For example, Zisselmar & Molerus (1979) found that, for a given particle size, the turbulence intensity at the centerline was reduced; but, close to the wall the turbulence intensity was increased for certain values of particle concentration. Tsuji *et al.* (1984) found cases where the turbulence intensity was increased on the centerline, but decreased near the wall.

COMPUTATION OF PRODUCTION AND DISSIPATION

The data of Tsuji *et al.* (1984), as depicted in figures 10 and 11, is used to estimate the excess turbulent energy due to the presence of the particles.

The particles were plastic spheres, 3 mm dia, $\rho_p = 1020\ \text{kg/m}^3$, with loading ratios 0.6, 2.3 and 3.4, which were suspended in air ($\rho_a = 1.18\ \text{kg/m}^3$; $\nu = 16 \times 10^{-6}\ \text{m}^2/\text{s}$) flowing in a vertical tube with a centerline velocity $\bar{u}_c$, and an average velocity $\bar{u}_m = 0.835\bar{u}_c$. The volumetric flow rates can be computed (e.g. for a loading of 3.4, $Q_a = 8.66 \times 10^{-3}\ \text{m}^3/\text{s}$; $Q_p = 3.41 \times 10^{-5}\ \text{m}^3/\text{s}$, the subscript a indicates air and p is for particles).

Unfortunately, the time-averaged relative velocities between the particles and the air were not explicitly given in the data and one has to estimate these from figure 10, and assume that the same relative velocity exists under the conditions of figure 11, which are somewhat different. Also, the relative velocity apparently is also dependent on the loading (it decreases as the loading increases). A numerical integration of the curves in figure 10 resulted in the relative velocity given in table 2. Based on the relative velocities, as listed in the table, the particle Reynolds numbers Re_p were computed, as well as the drag force F which acts on the particle (with a constant drag coefficient $C_D = 0.45$). Based on the particle velocity, the time of flight t_p of the particle through a unit length (say 1 m) of pipe was computed and then the total energy E_D which is dissipated by all the particles in a unit length of pipe was calculated (assuming that all the energy is due to the drag force). For example, with a loading of 3.4, the number of particles in a unit length of pipe is $n = 203$, $F = 6.53 \times 10^{-5}\ \text{N}$, $t_p = 0.17\ \text{s}$, $u_R = 5.9\ \text{m/s}$ and

$$E_D = n \times F \times u_R \times t_p = 13.1 \times 10^{-3}\ \text{J}.$$

One should notice that these calculations are approximate since they are based on a number of estimates from the given data.

The energy dissipated by the turbulent motion of the air can be estimated from

$$\varepsilon = 15\nu \frac{u_z^2}{\lambda^2},$$

where λ is a length scale, defined as

$$\lambda = \left(\frac{15}{A}\right)^{1/2} \frac{l_e}{\text{Re}^{1/2}},$$

where l_e is the length scale of the energy-containing eddies, estimated by Hutchinson *et al.* (1971) to be $0.2R$ (R—radius of the pipe); Re is the Reynolds number based on the fluctuating velocity in the axial direction $(\overline{u_z'^2})^{1/2}$; A is a parameter whose value is unknown for this case—and, for lack of better information, we shall set $A = 1$. For the current values, for $m = 0$, $\text{Re} = 180$,

Table 2. Effect of particles on turbulence [data from Tsuji *et al.* (1984)]

Loading ratio	0	0.6	2.3	3.4
Relative velocity $\bar{u}_R$ (m/s)	—	7.4	6.2	5.9
Particles' velocity $\bar{u}$ (m/s)	—	4.7	5.3	6.0
Particle Reynolds number Re_p	—	1388	1164	1106
Drag on a particle ($\text{N} \times 10^5$)	—	10.3	7.2	6.5
Energy spent on drag of particles ($\text{J} \times 10^3$)	—	5.6	12	13
Energy dissipation of turbulence ($\text{J} \times 10^3$)	20	40	50	71
Excess dissipation of turbulence ($\text{J} \times 10^3$)	—	20	30	51

$\lambda = 8.83 \times 10^{-4}$ m, $\varepsilon_{A,0} = 277$ m^2/s^3 and in a 1 m pipe $E_{T,0} = 20 \times 10^{-3}$ J; with a loading of $m = 3.4$, $\varepsilon_{A,3.4} = 979$ m^2/s^3 and $E_{T,3.4} = 71 \times 10^{-3}$ J, namely 51×10^{-3} J in excess of the case with no particles. This value is of the same order of magnitude as the amount of energy which was derived from the mainstream through the mechanism of vortex shedding (i.e. the drag on the particles).

For lack of better and more detailed data, one cannot claim an accuracy of the above estimates and one cannot adjust coefficients (say the A is the dissipation) to better fit the data.

CONCLUSIONS

The presence of particles with a low particle Reynolds number tends to suppress the turbulence of the carrier fluid. Particles with high particle Reynolds number (based on relative velocity and particle size), larger than about 400, tend to enhance the turbulence—most likely due to vortex shedding.

Additional experimental data are needed to quantify this effect.

Acknowledgements—Danny Kaftori's computations of the excess turbulence intensity are gratefully acknowledged. Professors Crow, Faeth, Lumley and Sreenivasan read the text and made some useful comments.

REFERENCES

ACHENBACH, E. 1974 Vortex shedding from spheres. *J. Fluid Mech.* **62,** 209–221.

AL TAWEEL, A. M. & LANDAU, J. 1977 Turbulence modulation in two-phase jets. *Int. J. Multiphase Flow* **3,** 341–351.

BESNARD, D., HARLOW, F. H. & RAVENZAHN, R. 1987 Conservative and transport properties of turbulence with large density variations. Report LA-10911-MS.

DANON, H., WOLFSHTEIN, M. & HETSRONI, G. 1977 Numerical calculations of two phase turbulent round jets. *Int. J. Multiphase Flow* **3,** 223–234.

FAETH, G. M. 1983 Recent advances in modeling particle transport properties and dispersion in turbulent flow. *Proc. ASME–JSME therm. Engng Conf.* **2,** 517–534.

FAETH, G. M. 1987 Mixing, transport and combustion in sprays. *Prog. Energy Combust. Sci.* **13,** 293–345.

GORE, R. & CROWE, C. T. 1989 Effects of particle size on modulating turbulent intensity. *Int. J. Multiphase Flow* **15,** 279–285.

HETSRONI, G. & SOKOLOV, M. 1971 Distribution of mass, velocity and intensity of turbulence in a two-phase turbulent jet. *Trans. ASME Jl appl. Mech.* **38,** 315–327.

HUTCHINSON, P., HEWITT, G. F. & DUKLER, A. E. 1971 Deposition of liquid or solid dispersion from turbulent gas streams: a stochastic model. *Chem. Engng Sci.* **26,** 419–439.

LEE, S. L. & DURST, F. 1980 On the motion of particles in turbulent flow. Report NUREG/CR-1554.

LEE, S. L. & DURST, F. 1982 On the motion of particles in turbulent duct flows. *Int. J. Multiphase Flow* **8,** 125–146.

LEVY, Y. & LOCKWOOD, F. C. 1981 Velocity measurements in a particle laden turbulent free jet. *Combust. Flame* **40,** 333–339.

MAEDA, M., HISHIDA, K. & FURUTANI, T. 1980 Optical measurements of local gas and particle velocity in an upward flowing dilute gas–solids suspension. In *Polyphase Flow and Transport Technology*, p. 211. Century 2-ETC, San Francisco, Calif.

MODARRESS, D., TAN, H. & ELGHOBASHI, S. 1984a Two-component LDA measurement in a two-phase turbulent jet. *AIAA Jl* **22,** 624–630.

MODARRESS, D., WUERER, J. & ELGHOBASHI, S. 1984b An experimental study of a turbulent round two-phase jet. *Chem. Engng Commun.* **28,** 341–354.

NOURI, J. M., WHITELAW, J. H. & YIANNESKIS, M. 1987 Particle motion and turbulence in dense two-phase flows. *Int. J. Heat Mass Transfer* **13,** 729–739.

ODAR, F. & HAMILTON, W. S. 1964 Force on a sphere accelerating in viscous fluid. *J. Fluid Mech.* **18,** 302–314.

OWEN, P. R. 1969 Pneumatic transport. *J. Fluid Mech.* **39,** 407–432.

PARTHASARATHY, R. N. & FAETH, G. M. 1987 Structure of a turbulent particle-laden water jet in still water. *Int. J. Multiphase Flow* **13,** 699–716.

RUCK, B. & MAKIOLA, B. 1989 Particle dispersion in a single-sided backward-facing step flow. *Int. J. Multiphase Flow* **14,** 787–800.

SERIZAWA, A. 1974 Fluid-dynamic characteristics of two-phase flow. Ph.D. Thesis, Kyoto Univ., Japan.

SERIZAWA, A. & KATAOKA, I. 1980 Fundamental aspects of the drift velocity in turbulent bubbly flow. *Tech. Rep. Inst. atom. Energy Kyoto Univ.*, No. 182.

SERIZAWA, A., KATAOKA, I. & MICHIYOSHI, I. 1975 Turbulence structure of air–water bubbly flow. *Int. J. Multiphase Flow* **2,** 221–259.

SHUEN, J. S., SOLOMON, A. S. P., ZHANG, Q-F. & FAETH, G. M. 1983 A theoretical and experimental study of turbulent particle-laden jets. Report NASA CR 168293.

SHUEN, J. S., SOLOMON, A. S. P., ZHANG, Q-F. & FAETH, G. M. 1985 Structure of particle-laden jets: measurements and predictions. *AIAA Jl* **23,** 396–404.

SNYDER, W. H. & LUMLEY, J. L. 1971 Some measurements of particle velocity autocorrelation functions in a turbulent flow. *J. Fluid Mech.* **48,** 41–71.

TSUJI, Y. & MORIKAWA, Y. 1982 LDV measurements of an air–solid two-phase flow in a horizontal pipe. *J. Fluid Mech.* **120,** 385–409.

TSUJI, Y., MORIKAWA, Y. & SHIOMI, H. 1984 LDV measurements of an air–solid two-phase flow in a vertical pipe. *J. Fluid Mech.* **139,** 417–434.

TSUJI, Y., MORIKAWA, Y., TANAKA, T., KARIMINE, K. & NISHIDA, S. 1988 Measurement of an axisymmetric jet laden with coarse particles. *Int. J. Multiphase Flow* **14,** 565–574.

WELLS, M. W. 1982 The effects of crossing trajectories on diffusion of particles in a turbulent fluid. Ph.D., Washington State Univ., Pullman.

WELLS, M. W. & STOCK, D. E. 1983 The effects of crossing trajectories on the dispersion of particles in turbulent fluid. *J. Fluid Mech.* **136,** 31–62.

WYGNANSKI, I. & FIEDLER, H. 1969 Some measurements in the self preserving jet. *J. Fluid Mech.* **38,** 577–612.

ZISSELMAR, R. & MOLERUS, O. 1979 Investigation of solid–liquid pipe flow with regard to turbulence modification. *Chem. Engng J.* **18,** 233.